

# The importance of the $V_p/V_s$ ratio in determining the error propagation, the stability and the resolution of linear AVA inversion: a theoretical demonstration

M. ALEARDI

*Earth Sciences Department, University of Pisa, Italy*

(Received: November 13, 2014; accepted: January 25, 2015)

**ABSTRACT** The linear Amplitude-Versus-Angle (AVA) inversion has become a standard tool in deep-sediments hydrocarbon exploration since its introduction in the oil and gas industry. However, in the last decades, with the increase of offshore construction activity, applications of this method have been also extended to predict overpressured zones and/or to evaluate the geotechnical properties of shallow sea bottom layers. Among the input parameters requested by linear AVA inversion there is the background  $V_p/V_s$  ratio across the reflecting interface and a  $V_p/V_s$  ratio of two is frequently assumed. This value is usually very close to the true ratio in case of deep, compacted sediments but it can be a gross underestimation of the true value in case of shallow or overpressured sediments. Despite that, the importance of the background  $V_p/V_s$  ratio in AVA inversion is frequently underrated and thus I consider two frequently used approximations of the Zoeppritz equations to study their impact on the outcomes of linear AVA inversion: the three-term Aki and Richards equation and the two-term Ursenbach and Stewart formula. These equations are then analysed, varying the  $V_p/V_s$  value, using tools frequently applied in sensitivity analysis. It turns out that the background  $V_p/V_s$  ratio controls the error propagation from data to model space and determines the cross-talk between the inverted parameters. Moreover, an increasing  $V_p/V_s$  ratio causes a decrease of stability of the AVA inversion and worsens the estimate of the  $V_s$  contrast at the reflecting interface.

**Key words:** AVA inversion,  $V_p/V_s$  ratio.

## 1. Introduction

Amplitude-Versus-Angle (AVA) methods exploit the variation in seismic reflection amplitudes with increasing incidence angle to infer the contrasts in seismic velocities and densities at the reflecting interfaces (Castagna *et al.*, 1998). For this characteristic, AVA techniques have been extensively used worldwide for lithology and fluid prediction in hydrocarbon exploration (e.g., Ostrander, 1984; Rutherford and Williams, 1989; Mazzotti, 1990, 1991; Grion *et al.*, 1998; Mazzotti and Zamboni, 2003).

Most AVA methods are based on the Zoeppritz equations (Zoeppritz, 1919) which describe the variation in seismic amplitude with increasing angle of incidence for a plane wave incident

on an interface separating two semi-infinite half spaces. The system of equations formulated by Zoeppritz is algebraically complex and many different approximated formulas have been derived to simplify and linearise the inversion. These simplified equations, valid under certain assumptions, are those frequently used in AVA inversion and interpretation (Wang, 1999; Ursenbach and Stewart, 2008).

Performing linear AVA inversion, an average  $V_p/V_s$  ratio across the interface equal to two is usually assumed (Castagna *et al.*, 1998). This ratio is a good approximation for classical deep hydrocarbon exploration, but generally it is an underestimation of the true average ratio in case of seabed sediments. Therefore, this approximation may constitute a source of errors when AVA inversion is used for investigating shallow layers which are usually characterized by high  $V_p/V_s$  ratios. In particular, due to the increase of offshore construction activity in marine areas, a reliable characterization of shallow sediments is of great interest (Theilen and Pecher, 1990; Ayres and Theilen, 1999). For this, to identify safe zone where installing underwater structures, the outcomes derived from AVA method are frequently used for shallow hazard assessment and well site analysis (Riedel and Theilen, 2001). In these exploration phases the elastic properties derived from AVA inversion (P- and S-wave velocities and bulk density) are often converted into geotechnical properties (e.g., shear strength and elastic moduli) needed for engineering purposes.

Therefore, in this work I want to assess the impact of the assumed  $V_p/V_s$  ratio on the expected resolution and uncertainties associated with each inverted parameter. To this end, I analyze the three-term Aki and Richards (Aki and Richards, 1980) equation and the two-term Ursenbach and Stewart equation (Ursenbach and Stewart, 2008), making use of the sensitivity analysis tools applied to the inversion kernel. Firstly, I study how the  $V_p/V_s$  value influences the condition number, the magnitude of the eigenvalues and the orientation of associated eigenvectors in model space, then, studying the model resolution and covariance matrices, I analyze how the  $V_p/V_s$  ratio determines both the expected resolution of each inverted parameter and the error propagation from data space to model space.

## 2. Inverse problems, sensitivity analysis and SVD decomposition

A seismic inverse problem aims to estimate model parameters ( $m$ ) from collected data ( $d$ ) minimizing the misfit between predicted and observed data (Tarantola, 2005). If we assume that the fundamental physics is adequately understood, a function  $G$ , may be specified relating  $m$  and  $d$ :

$$d = G(m) \quad (1)$$

The simplest inverse problems are those that can be represented by an explicit linear equation  $d = Gm$ , where  $G$  takes a matrix form. Many important seismic inverse problems are linear, such as the AVA inversion performed by applying approximations of the Zoeppritz equations. One commonly used measure of misfit between observed data and modelled data in solving an inverse problem is the  $L_2$  norm of the residuals. A model that minimizes this  $L_2$  norm is called a least-squares solution. The least-squares solution for linear inverse problems can be derived using the following equation (also called the normal equations solution):

$$m_{L_2} = (G^T G)^{-1} G^T d \quad (2)$$

where the superscript  $T$  indicates the transpose. In a compact form, the solution of a linear inverse problem can be written as follow:

$$m = G^{-g} d \quad (3)$$

where  $G^{-g}$  is called the generalized inverse. For a common overdetermined least-squares problem, this matrix is equal to:

$$G^{-g} = (G^T G)^{-1} G^T \quad (4)$$

However, to solve an inversion problem, one must not only find a solution that best fits the observed data but should also investigate the relation between the estimated model and the true model or, in other words, analyze which properties of the true model are resolved in the estimated model. This issue can be approached with the sensitivity analysis method. For linear inverse problems this analysis essentially consists in computing the model covariance and model resolution matrices. The model resolution matrix ( $R$ ) describes how well the predicted model matches the true one. It can be demonstrated (Aster *et al.*, 2005) that the resolution matrix for a linear inverse problem can be computed as follows:

$$R = G^{-g} G \quad (5)$$

If  $R$  is equal to an identity matrix each model parameter is perfectly resolved and uniquely determined. When  $R$  is not equal to the identity matrix some part of the problem is not perfectly resolved and the final solution is also influenced by the off-diagonal terms [see Aster *et al.* (2005) for a complete discussion]. To understand how an error in the data propagates as an error in the estimated model, it is useful to define the model covariance matrix ( $C_m$ ). If the data are assumed to be uncorrelated and all have equal variance, the covariance matrix (unit covariance matrix) is given by:

$$C_m = G^{-g} G^{-gT} \quad (6)$$

The unit covariance matrix is a measure of how uncorrelated noise with unit variance in the data is mapped into uncertainties in the estimated model parameters. The diagonal terms indicate the variance associated with each model parameter, whereas the off-diagonal terms indicate covariances. The model resolution and model covariance matrices are functions of only the data kernel (the  $G$  matrix in Eq. 1) and the a-priori information added to the problem.

Another useful tool in approaching inverse problems is the Singular Value Decomposition (SVD). According to this method the matrix  $G$  is broken down into the product of three matrices:

$$G = USV^T \quad (7)$$

where  $S$  is a diagonal matrix of singular values,  $V$  is the matrix of eigenvectors in model space and  $U$  contains the eigenvectors in data space. The SVD decomposition is essential in sensitivity analysis because it permits to get a better understanding of the physical meaning of the  $G$  matrix. Moreover, the SVD method is also a powerful tool for solving ill-conditioned least-squares problems. In these problems, the process of computing an inverse solution is extremely unstable and a small change in the measurements can lead to a large change in the estimated model. In these cases the  $G$  matrix is characterized by a high condition number, which is the ratio between the highest and the smallest singular values of the  $G$  matrix. Therefore, in order to stabilize the inversion, the Truncated SVD method (T-SVD) can be applied. This method is aimed at eliminating the smallest singular values of the  $G$  matrix and at reducing the condition number. We pay a price for this stability in that the regularized solution has a decreased resolution. Very detailed information about geophysical inverse problems can be found in Aster *et al.* (2005) and Tarantola (2005).

### 3. The Aki and Richards and Ursenbach and Stewart approximations

Starting from the Zoeppritz equations, Aki and Richard (1980) provided approximation for P-P wave reflection coefficients that is valid for small physical contrasts and small incidence angles (generally less than 30-35 degrees). This equation can be written as

$$R_{pp}(\theta) = \frac{1}{2\cos^2\theta} \frac{\Delta\alpha}{\bar{\alpha}} - 4\gamma^2 \sin^2\theta \frac{\Delta\beta}{\bar{\beta}} - \frac{1}{2} (4\gamma^2 \sin^2\theta - 1) \frac{\Delta\rho}{\bar{\rho}} \tag{8}$$

where  $R_{pp}$  is the P-wave reflection coefficient,  $\theta$  is the average of P-wave incidence and P-wave transmission angles across the interface, and  $\alpha$ ,  $\beta$ , and  $\rho$ , indicate the P-wave velocity, S-wave velocity and density, respectively. In Eq. 8,  $\Delta x$  is the difference of property  $x$  across the reflecting interface ( $x_2-x_1$ ) and indicates the average property across the interface  $(x_2+x_1)/2$ , whereas  $\gamma$  is the reciprocal of the background  $Vp/Vs$  ratio:

$$\gamma = \frac{\beta_1 + \beta_2}{\alpha_1 + \alpha_2} \tag{9}$$

where the subscripts 1 and 2 refer to the overlying and underlying media, respectively.

The Aki and Richards equation is inverted to retrieve the relative contrasts at the reflecting interface that can be conveniently written as

$$\frac{\Delta\alpha}{2\bar{\alpha}} = R_p; \quad \frac{\Delta\beta}{2\bar{\beta}} = R_s; \quad \frac{\Delta\rho}{2\bar{\rho}} = R_\rho \tag{10}$$

In this form  $R_p$ ,  $R_s$  and  $R_\rho$  indicate the P-wave, S-wave and density reflectivity, respectively.

To reduce the physical ambiguity inherent to the AVA method (Drufuca and Mazzotti, 1995) and to stabilize the inversion process, the number of unknowns can be reduced. To this end two-term approximations of the Zoeppritz equations are frequently used. In particular in this work I consider the Ursenbach and Stewart equation (Ursenbach and Stewart, 2008):

$$R_{pp}(\theta) = \left( 1 + \frac{4\gamma^2 \cos^2\theta - 1}{5} \sin^2\theta \right) \frac{R_I}{\cos^2\theta} - 8\gamma^2 \sin^2\theta R_J \tag{11}$$

where the density term is incorporated into the P and S-impedance relative contrasts at the reflecting interface expressed by  $R_I$  and  $R_J$ , respectively:

$$\frac{\Delta Ip}{2\bar{I}p} = R_I; \quad \frac{\Delta Is}{2\bar{I}s} = R_J; \tag{12}$$

where  $Ip$  and  $Is$  represent the P and S-impedance, respectively.

These linear approximations of the Zoeppritz equations enable the description of the relationship between the observed AVA response ( $R_{pp}$ ) and the model parameters ( $m$ ) in a linear, compact, matrix form:

$$R_{pp}(\Theta) = Gm \tag{13}$$

In this form the  $G$  matrix contains the three- or the two-term equation, whereas the vector  $m$  contains the inverted parameters (elastic or impedance contrasts at the reflecting interface).

The singular value decomposition of the  $G$  matrix ( $G=USV^T$ ; see Eq. 7) splits the reflectivity  $R_{pp}(\theta)$  into three orthogonal components in both data space and model space.

The energy of each component is given by the corresponding eigenvalue. If the orders of magnitude of the eigenvalues are significantly different from each other, then a high signal-to-noise ratio is needed to estimate the signal in the low-energy directions. It is interesting to consider the physical meaning of the decomposition. The eigenvectors  $V$  are a basis in the model space. The eigenvalues  $S$  represent the reflected energy due to medium perturbations along the eigenvectors in model space. The amplitude versus angle effects of the reflections are described by the eigenvectors in data space ( $U$ ), which are three orthogonal functions (De Nicolao *et al.*, 1993).

#### 4. Condition number, eigenvalues and eigenvectors in model space

I now compare the condition number for the three- and the two-term inversions by varying the background  $V_p/V_s$  ratio (in all the following considerations when referring to a  $V_p/V_s \gg 2$  a  $V_p/V_s$  ratio equal to 8 is assumed). I remind that high condition numbers indicate an ill-conditioned problem. Therefore, I can determine how the  $V_p/V_s$  ratio influences the stability of the inverse problem. The threshold of stability of linear AVA inversion can be approximately established at a condition number between 200 and 500 (around -40 to -50 dB). If we fix this threshold at 300 (dashed line in Fig. 1), we can see that in case of  $V_p/V_s=2$  (or  $V_s/V_p=0.5$ , a common ratio used in deep sediment exploration), the inverse problem becomes stable as we pass from the three-term approximation (red curve in Fig. 1) to the two-term approximation (blue curve in Fig. 1). Conversely, when the  $V_p/V_s$  ratio is very high (or  $V_s/V_p$  approaches 0), as it occurs for shallow or seabed sediments, the inverse problem is ill-conditioned even if a two-term approximation is considered. Therefore, in the case of linear AVA inversion with very high  $V_p/V_s$  ratios, a regularization is needed to stabilize the inversion. A common method used for this purpose is the truncated singular value decomposition (T-SVD) that consists in the suppression of the smallest singular values of the  $G$  matrix.

Let us consider the sensitivity analysis, reminding that the threshold of stability ranges between 200 and 500. I start with the three-term Aki and Richards equation. Fig. 2 shows the singular values of the  $G$  matrix, where we can see that, independently from the  $V_p/V_s$  ratio, the first singular value contains almost all of the signal energy; the second one is negligible for small incidence angles and, although it increases at higher angles, is always 15-20 dB below the first singular value. The third singular value is very small for all of the angle range and, in practical cases, will be covered by noise and should be eliminated to stabilize the inversion. These results evidence that for both  $V_p/V_s=2$  and  $V_p/V_s \gg 2$ , only one linear combination of parameters (the combination that corresponds to the first eigenvector) can be reliably estimated at low angles. The estimation of two independent combinations (the first and second eigenvector) requires wider angles and is characterized by a poorer signal-to-noise ratio in the direction of the second singular value. The estimation of three independent combinations of parameters is clearly an ill-conditioned problem. Concerning the effect of the background  $V_p/V_s$  on the stability of the inversion, we can compare the results for  $V_p/V_s=2$  (Fig. 2a) with those for  $V_p/V_s \gg 2$  (Fig. 2b): the values associated with the second and third singular values decrease as the  $V_p/V_s$  ratio increases and this fact explains why the stability of the inversion decreases for increasing  $V_p/V_s$  ratios.

Fig. 1 - Condition number for the three-term Aki and Richards equation (red line) and the two-term Ursenbach and Stewart equation (blue line) for varying background  $V_s/V_p$  ratios. The dotted line represents the assumed threshold of stability for the linear AVA inversion.

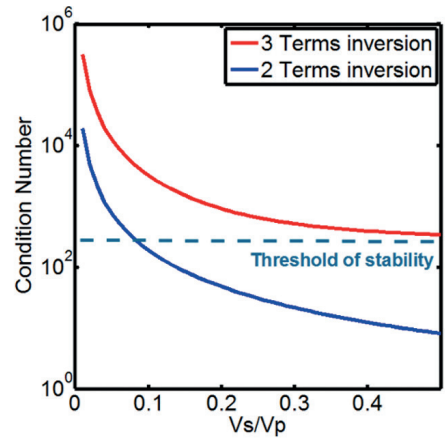


Fig. 2 - Singular values of the  $G$  matrix for the three-parameter inversion. Panels a and b correspond to  $V_p/V_s = 2$  and  $V_p/V_s \gg 2$ , respectively. For each case, the first, second and third singular value are represented from top to bottom.

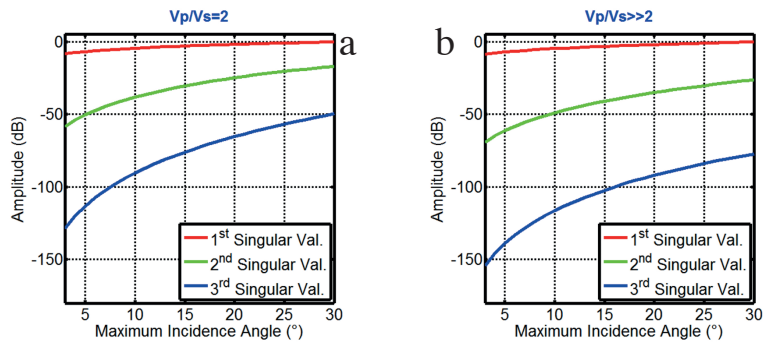
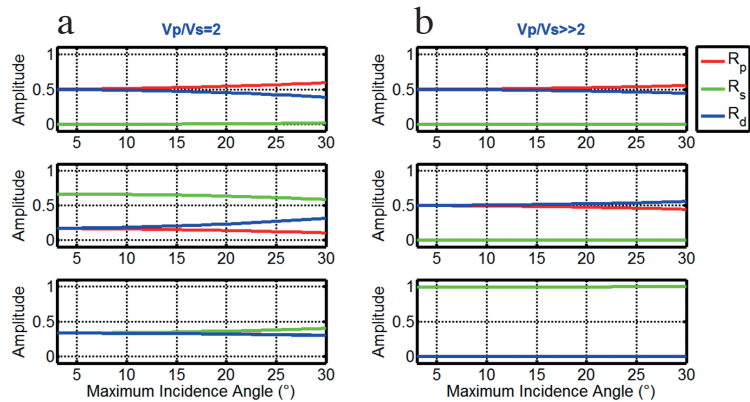


Fig. 3 - Eigenvectors in model space versus the maximum incidence angle for three-term inversion. Panels a and b correspond to  $V_p/V_s = 2$  and  $V_p/V_s \gg 2$ , respectively. For each case, the first, second and third eigenvector are represented from top to bottom.



Now I move on to describe the orientation of the eigenvectors in model space for the three-term inversion. Firstly, I analyze the Aki and Richards equation assuming a  $V_p/V_s$  ratio of two (Fig. 3a). For low angles, the  $R_p$  and  $R_d$  components are equal and  $R_s$  is zero. Therefore, the vector points in the direction of P-impedance perturbations. This result is obvious: it is known that the normal incidence reflection coefficient depends on the acoustic impedance contrast only. The  $R_s$  component becomes significant for higher angles. The second eigenvector points, approximately, in the direction of S-impedance perturbations, whereas the third eigenvector is difficult to interpret because it depends by a combination of different perturbations and does not have any particular physical meaning.

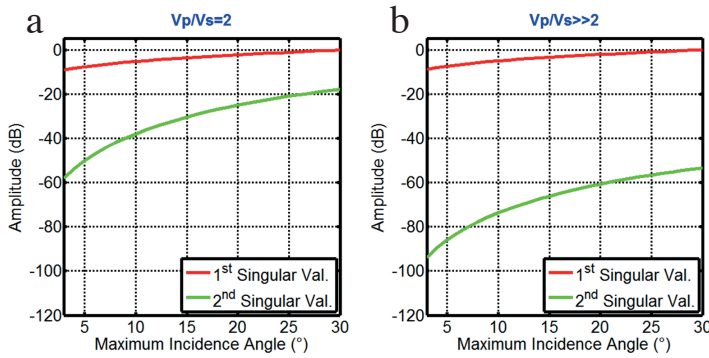


Fig. 4 - Singular values of the  $G$  matrix for two-parameter inversion. Panels a and b represent the  $V_p/V_s=2$  and  $V_p/V_s \gg 2$  cases, respectively

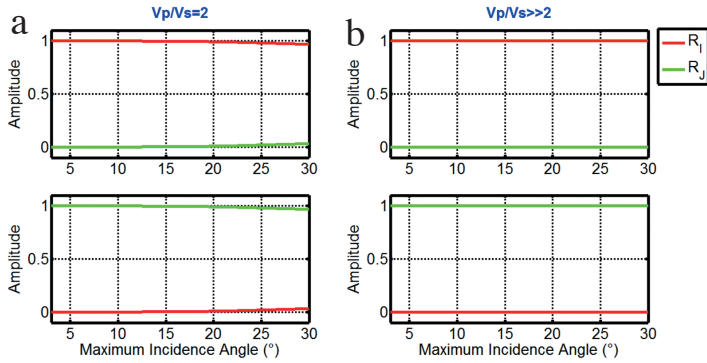


Fig. 5 - Eigenvectors in model space versus the maximum incidence angle for two-term inversion. Parts a and b correspond to  $V_p/V_s=2$  and  $V_p/V_s \gg 2$ , respectively. For each case, the first and second eigenvector are represented from top to bottom.

In the  $V_p/V_s \gg 2$  case (Fig. 3b), both the first and second eigenvectors, associated with the first and second singular values, point toward the P-impedance. Conversely, only the third eigenvector, associated with the smallest singular value, points entirely in the  $R_s$  direction. This fact indicates that this component spans the null-space of the  $G$  matrix and thus the S-wave velocity plays a very minor role in determining the AVA response. Moreover, by comparing the first and second eigenvectors for  $V_p/V_s=2$  and  $V_p/V_s \gg 2$ , we can see that an increased  $V_p/V_s$  ratio increases the cross-talk between the P-velocity term  $R_p$  and the density term  $R_d$ : a smaller distance is observed between the  $R_p$  and  $R_d$  components as the  $V_p/V_s$  ratio increases. This indicates that an independent estimation of these two parameters is more problematic in the case of high  $V_p/V_s$  values. These observations allow us to draw some important conclusions. First, the difficulty of achieving a reliable  $R_s$  estimation with increasing  $V_p/V_s$  values; second, the cross-talk between  $R_p$  and  $R_d$  also increases as the  $V_p/V_s$  ratio increases.

Let us now consider the sensitivity analysis for the two-term Ursenbach and Stewart equation. Based on the singular values of the  $G$  matrix (Fig. 4), it is clear that the stability of the problem is again influenced by the  $V_p/V_s$  ratio, confirming the observation made on the condition number (Fig. 1): the two-term linear AVA inversion becomes stable if the  $V_p/V_s$  value is sufficiently low.

For what concerns the eigenvectors in model space for the two-term approximation we can see that in the case of  $V_p/V_s=2$  (Fig. 5a), the first eigenvector points toward the P-impedance for small angles, whereas the  $R_j$  component is not null only if large incidence angles (greater than 20 degrees) are considered. Conversely, if we increase the  $V_p/V_s$  ratio (Fig. 5b), the first eigenvector points toward the P-impedance for the entire angular range. In this case, the  $R_j$  parameter spans the null space of the  $G$  matrix, indicating that, to try estimating the  $R_j$  term, a sufficiently low  $V_p/V_s$  ratio is needed. Note that the two-term inversion is stable for sufficiently low  $V_p/V_s$  values only (see Fig. 1), and in these cases, the use of the second eigenvector allows the inversion to

extract the  $R_j$  parameter. In the  $Vp/Vs=2$  case, this eigenvector can be used in the inversion and the  $R_j$  information can be recovered with a good degree of accuracy. Instead, in cases of  $Vp/Vs \gg 2$ , to stabilize the inversion the truncation of the second singular value (and the associated eigenvector) is needed and this renders the estimation of  $R_j$  impossible.

## 5. Model resolution and unit covariance matrices

The model covariance and resolution matrices describe how the error in the data space propagates in the model space and how well the estimated parameters match the true ones, respectively. I start by analyzing the unit covariance matrix (computed by assuming an identity data covariance matrix) for the least-squares inversion, for which the model resolution matrix is equal to an identity matrix [see Aster *et al.* (2005) for a rigorous mathematical demonstration].

Fig. 6 shows the unit covariance matrices computed for  $Vp/Vs=2$  (Figs. 6a and 6c) and  $Vp/Vs \gg 2$  (Figs. 6b and 6d) and for both the three- and two-term approximations. Note that the order of magnitude of the errors decreases passing from the three- to two-term inversion (for any background  $Vp/Vs$  value), and passing from  $Vp/Vs \gg 2$  to  $Vp/Vs=2$ , for both parametrizations. Also note that the  $Vp/Vs$  ratio determines the amount and the distribution of error propagation from the data to the model space. In fact, for high  $Vp/Vs$  values (Figs. 6b and 6d), the parameters most contaminated by noise are those associated with the S-wave velocity ( $R_s$  and  $R_j$ ). Instead, if the  $Vp/Vs$  is equal to two (Figs. 6a and 6c), the error is more homogeneously distributed although, even in this case, the error most strongly affects  $R_s$  and  $R_j$ .

Now I eliminate the smallest singular value of the  $G$  matrix (applying the T-SVD method) and recompute the unit covariance and the model resolution matrices. Let us first consider the model resolution matrices (Fig. 7). For the three-term inversion and in the case of  $Vp/Vs=2$ , the three parameters can be recovered with almost the same resolution, even if the lowest resolution is always related to  $R_s$  (Fig. 7a). Conversely, it is clear that for the  $Vp/Vs \gg 2$  case (Fig. 7b) we obtain a null resolution for the  $R_s$  parameter and a good resolution for both  $R_p$  and  $R_d$  (note that the resolution is expressed by the diagonal terms). If we reduce the dimension of the model space considering the two-term equation, we can see that for both cases (Figs. 7c and 7d), the  $R_j$  parameter is characterized by the highest resolution. Also in this case, the resolution of the  $Vs$ -related parameter  $R_j$  decreases with the increasing  $Vp/Vs$  ratio.

Now I describe the unit covariance matrix, which is obtained after applying the T-SVD method (Fig. 8) to eliminate the smallest singular value of the  $G$  matrix and to stabilize the inversion. I start with the three-term inversion. For high  $Vp/Vs$  ratios (Fig. 8b), the error is mapped onto the  $R_p$  and  $R_d$  parameters because the third eigenvalue, pointing toward the  $R_s$  parameters, has been eliminated by the truncation. We also observe a strong negative covariance (expressed by the off-diagonal terms and indicating a correlation) between  $R_p$  and  $R_d$ , which confirms the strong cross-talk between these two unknowns and the difficulties of achieving an independent estimation. As expected, both the correlation between  $R_p$  and  $R_d$  and the error magnitude decrease if we consider a  $Vp/Vs$  ratio equal to two (Fig. 8a). In this case, the error is more homogeneously distributed among the three parameters. Also by observing the unit-covariance matrix for the two-term inversion, we see that the error magnitude decreases from the  $Vp/Vs \gg 2$  (Fig. 8d) case to the  $Vp/Vs=2$  case (Fig. 8c). Moreover, the truncation of the

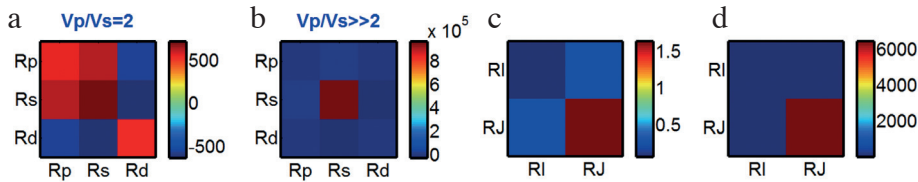


Fig. 6 - Unity covariance matrices in the case of a least-squares inversion. Panels a and c represent the  $V_p/V_s = 2$  case and the associated three- and two-term inversions, whereas the  $V_p/V_s \gg 2$  case and the associated three- and two-term inversions are shown in panels b and d.

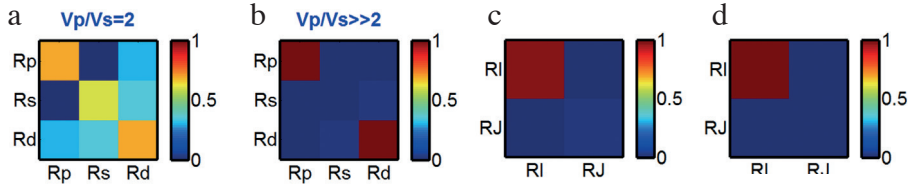


Fig. 7 - Model resolution matrices after applying the T-SVD method. Panels a and c represent the  $V_p/V_s = 2$  case and the associated three- and two-term inversions, whereas the  $V_p/V_s \gg 2$  case and the associated three- and two-term inversions are shown in panels b and d.

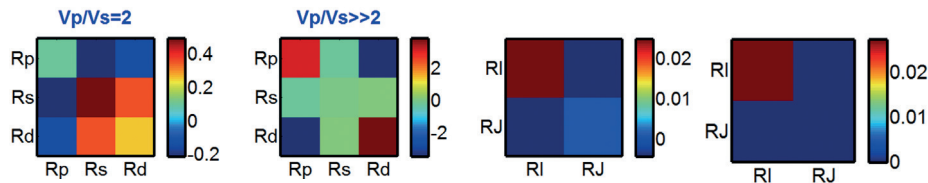


Fig. 8 - Unit covariance matrices after applying the T-SVD method. Panels a and c represent the  $V_p/V_s = 2$  case and the associated three- and two-term inversions, whereas the  $V_p/V_s \gg 2$  case and the associated three- and two-term inversions are shown in panels b and d.

second singular values (in the case of  $V_p/V_s \gg 2$ ) results in the error being mapped entirely onto the  $R_I$  parameters, whereas in the case of  $V_p/V_s = 2$ , the error also affects the  $R_J$  values. Finally, by comparing Figs. 6 and 8, we can see that in any case the T-SVD method reduces the order of magnitude of the error associated with each parameter estimation.

## 6. Conclusions

The sensitivity analysis highlights the strong influence of the background  $V_p/V_s$  ratio on both the stability of the linear AVA inversion and on the physical meaning expressed by the  $G$  matrix. Specifically, I have analyzed how the  $V_p/V_s$  value influences the condition number, the orientation of eigenvectors in model space, the resolution for each inverted parameter and the error propagation from data to model space. From the analysis of the condition number, I note that if  $V_p/V_s$  is equal to 2 the inverse problem becomes stable as I pass from the three-term (contrasts in P-wave velocity, S-wave velocity and density) to the two-term (contrasts in P-wave and S-wave impedances) approximation. Conversely, when the  $V_p/V_s$  ratio is very high (as occurs for overpressured or shallow seabed sediments), the inverse problem is ill-conditioned even if a two-term approximation is considered. Therefore, in the case of linear AVA inversion with very high  $V_p/V_s$  ratios, the application of a regularization method (i.e., the T-SVD method) is needed to stabilize the inversion process. Moreover, the orientation of the eigenvectors in

model space shows that for high  $V_p/V_s$  ratios the eigenvectors associated with the  $V_s$ -related parameter ( $R_s$  and  $R_f$ ) span the null-space of the inversion kernel. This fact, combined with the observation of the resolution matrices, highlights that the determination of the  $V_s$  contrast (or the S-impedance contrast) for shallow sediments or at sea bottom becomes a hopelessly non-unique problem in the case of high  $V_p/V_s$  values. Finally, I observe that when increasing the  $V_p/V_s$  values the error propagation from data to model space becomes more and more severe. The same happens to the cross-talk between  $R_p$  and  $R_d$ , making their independent estimation impossible.

Therefore, it emerges that linear AVA inversion is not suitable to investigate under-consolidated or overpressured sediments that are usually characterized by very high  $V_p/V_s$  ratios. In those cases, it is likely that non linear and wide-angle inversion approaches are needed.

#### REFERENCES

- Aki K. and Richards P.G.; 1980: *Quantitative seismology: theory and methods*. WH Freeman, San Francisco, CA, USA, vol. 1 and 2, 557 and 373 pp.
- Aster R.C., Borchers B. and Thurber C.H.; 2005: *Parameter estimation and inverse problems*. Elsevier Academic Press, London, England, 296 pp.
- Ayres A. and Theilen F.; 1999: *Relationship between P- and S-wave velocities and geological properties of near-surface sediments of the continental slope of the Barents Sea*. Geophys. Prospect., **47**, 431-441.
- Castagna J.P., Swan H.W. and Foster D.J.; 1998: *Framework for AVO gradient and intercept interpretation*. Geophys., **63**, 948-956.
- De Nicolao A., Drufuca G. and Rocca F.; 1993: *Eigenvalues and eigenvectors of linearized elastic inversion*. Geophys., **58**, 670-679.
- Drufuca G. and Mazzotti A.; 1995: *Ambiguities in AVO inversion of reflections from a gas-sand*. Geophys., **60**, 134-141.
- Grion S., Mazzotti A. and Spagnolini U.; 1998: *Joint estimation of AVO and kinematic parameters*. Geophys. Prospect., **46**, 405-422.
- Mazzotti A.; 1990: *Prestack amplitude analysis methodology and application to seismic bright spots in the Po Valley, Italy*. Geophys., **55**, 157-166.
- Mazzotti A.; 1991: *Amplitude, phase and frequency versus offset applications*. Geophys. Prospect., **39**, 863-886.
- Mazzotti A. and Zamboni E.; 2003: *Petrophysical inversion of AVA data*. Geophys. Prospect., **51**, 517-530.
- Ostrander W.; 1984: *Plane-wave reflection coefficients for gas sands at non-normal angles of incidence*. Geophys., **49**, 1637-1648.
- Riedel M. and Theilen F.; 2001: *AVO investigations of shallow marine sediments*. Geophys. Prospect., **49**, 198-212.
- Rutherford S.R. and Williams R.H.; 1989: *Amplitude-versus-offset variations in gas sands*. Geophys., **54**, 680-688.
- Tarantola A.; 2005: *Inverse problem theory and methods for model parameter estimation*. Soc. Ind. Appl. Math., Philadelphia, PA, USA, 342 pp., doi:10.1137/1.9780898717921.
- Theilen F. and Pecher I.A.; 1990: *Assessment of shear strength of the sea bottom from shear wave velocity measurements on box cores and in-situ*. In: Hovem J.M., Richardson M.D. and Stoll R.D. (eds), *Shear Waves in Marine Sediments*, Kluwer Academic Publishers, Dordrecht, the Netherlands, pp. 41-49.
- Ursenbach C.P. and Stewart R.R.; 2008: *Two-term AVO inversion: equivalences and new methods*. Geophys., **73**, 31-38.
- Wang Y.; 1999: *Approximations to the Zoeppritz equations and their use in AVO analysis*. Geophys., **64**, 1920-1927.
- Zoeppritz K.; 1919: *Erdbebenwellen VII*. Nachrichten von der Gesellschaft der Wissenschaften zu Göttingen, Mathematisch-Physikalische Klasse, 57-65.

Corresponding author: Mattia Aleardi  
 Dipartimento di Scienze della Terra, Università  
 Via Santa Maria 53, 56126 Pisa, Italy  
 Phone: +39 050 221; fax: +39 050;  
 email: mattia.aleardi@for.unipi.it